

# Quantitative evaluation of strain effects in STEM HAADF contrast

V. Grillo\*

National Research Center S3, CNR-INFM Via Campi 213/A, 41100 Modena; Laboratorio Nazionale TASC INFM-CNR, Area Science Park, S. S. 14, Km 163.5, 34012 Trieste, Italy

\*Vincitore del Premio SISM 2008

Corresponding author: Vincenzo Grillo

National Research Center S3, CNR-INFM Via Campi 213/A, 41100 Modena, Italy

Tel: +39.059.2055259 - Fax: +39.059.2055651

E-mail: grillo@tasc.infm.it

## Summary

In the context of the methodological studies aimed to give a quantitative evaluation of composition basing on High Angle Annular Dark Field (HAADF) STEM imaging, I propose to afford quantitatively the effect of a strain field varying along the electron propagation direction. I propose, as a case study, the well known surface strain relaxation in a STEM specimen comprising an InGaAs-GaAs Quantum Well. I will demonstrate, by means of experiments and simulation that, surface strain relaxation produce characteristic intensity dips at the sides of the QW not ascribable to chemical effects. The origin of this contrast will be correlated with the characteristic phenomenon of channelling in zone axis conditions.

**Keywords:** HAADF, surface strain relaxation, channeling.

## Introduction

The methodological research aimed to produce quantitative analysis based on high-resolution transmission electron microscopy (HRTEM) has reached, under many aspects, a good degree of maturity as many effects concurring to the image formation have been clarified (Coene *et al.*, 1992; Van Dyck and Op de Beeck, 1996; Kret *et al.*, 2001). On the contrary, in many cases, the use Scanning Transmission Electron Microscopy (STEM) technique with High Angle Annular Dark Field (HAADF) detector mainly remains qualitative as new methods to give a quantitative interpretation of HAADF images are still being developed (Anderson *et al.*, 1997; Liu *et al.*, 1999; Carlino and Grillo, 2005; Grillo and Carlino, 2008; LeBeau *et al.*, 2008). One of the main advantages of the technique is indeed its capacity to make evident a compositional variation through a change of the intensity. This is particularly appealing in the case of imaging in low index zone axis conditions for which the chemical information on a single atomic column can be readily obtained.

The strong compositional sensitivity is also related to the use of a large collection angle. Indeed for a sufficiently large scattering angle the scattering contribution is dominated, at room temperature, by the thermal diffuse scattering (TDS). One of the peculiarities of this scattering mechanism (but also of the elastic contribution at high angle (Rafferty *et al.*, 2001)) is that the scattering contributions of atoms sum incoherently with each other (Pennycook and Jesson, 2001). This is quite different from what happens with HRTEM images where the interference of the coherent scattering from each atom needs to be considered. This highly coherent nature of the HRTEM image formation makes it intrinsically more sensible to any non-periodic effect of the crystalline structure and in particular to the strain fields. Such effects superimpose and often dominate on compositional effects (Ruvinov *et al.*, 1995; De Caro *et al.*, 1997). It results therefore evident the advantage of an incoherent technique as HAADF for its possibility to reduce strain related effects. Experimentally it is indeed observed a drastic reduction of such effects when the detector inner aperture is increased (Hillyard and

Silcox, 1995; Yu *et al.*, 2004).

For sufficiently high inner angle of the detector the simplest approach for interpreting HAADF imaging assumes the intensity to be the convolution of a function representing the probe at the entrance of the specimen and a function accounting for the scattering by the atomic columns (Anderson *et al.*, 1997). In practice this is equivalent to assume that a TDS wave is produced at each atomic position with intensity proportional to the intensity of the impinging beam at that position. The success of this assumption is, in most cases, relatively good. This makes the HAADF imaging in zone axis conditions a valid instrument for the analysis of the atomic positions in complex structures (interfaces defects and so on) (Xin *et al.*, 1998; Lopatin *et al.*, 2002; Klenov *et al.*, 2005). In spite of this success this simplified scheme may be inadequate for the prediction of finer effects in the HAADF contrast, starting from the intensity dependence on thickness, the effect of static displacement (this has been already considered in a previous article (Grillo and Carlino, 2008)) or of strain that will be the object of this work. In particular these effects show up most importantly right in the low order zone axis conditions where the technique shows most of its advantages. It is worth mentioning that these fine effects cannot be completely eliminated even with the use of a large angle. Their evaluation becomes therefore necessary whenever accurate quantitative chemical information need to be extracted from the HAADF images. In these cases the use of simulations becomes mandatory for a correct image interpretation and quantification.

It is, at this point, interesting to briefly discuss the origin of the deviations from the simple image interpretation. Interestingly the incoherent nature of the TDS waves remains valid to a very good degree of approximation. Conversely the most important pitfall of the simple convolution model is that it does not take into account the interaction of the electron beam with the sample. Specifically in the case of zone axis conditions a narrow probe excites predominantly the columnar Bloch states (also named 1s) and several less localized states (Anderson *et al.*, 1997). The large excitation of the 1s states is also referred to as channelling. The actual wavefunction inside the sample is the result of the interference of all these Bloch states. The first evidence of this phenome-

non is visible for example in the oscillation of the derivative of the intensity with specimen thickness (Voyles *et al.*, 2003).

A more indirect evidence of this arises from the calculation and observation of the dependence on mistilt of the HAADF intensity. Small tilts off the zone axis condition have the effect to reduce the average HAADF intensity in a unit cell while leaving the atomic fringe pattern almost unchanged (Maccagnano-Zacher *et al.*, 2008). This reduction becomes even more evident when passing from crystalline to amorphous materials (Yu *et al.*, 2008). These evidences have convincingly demonstrated that the preferential propagation of electrons along highly symmetric directions strongly affects the HAADF average intensity. As a consequence of these observations it can be predicted that any perturbation of the columnar order and in particular strain effects can produce contrast in HAADF images. While these effects are often neglected in literature, in a few significant cases evidences for strain related contrast in HAADF have been shown (Treacy *et al.*, 1985; Cowley and Huang, 1992; Perovic *et al.*, 1993; Amali *et al.*, 1997; Liu *et al.*, 2001; Fitting *et al.*, 2006).

Two kinds of mechanisms have been claimed to be involved in the formation of the HAADF strain contrast. The first, sometimes referred to as Huang scattering, is related to the increase of the diffuse scattering at high angles as an effect of the increased static disorder. This mechanism has been claimed to be at the origin of the intensity increase of both high angle transmission electron microscopy and, to less extent, HAADF in proximity of dislocations (Wang 1994). The second mechanism is related to dechannelling, namely the reduction of the 1s contribution to the electron wavefunction due to interband scattering between Bloch waves, induced by local strain. Strain indeed produces a faster depletion of the states localized to the atomic columns in favour of less localised states (Cowley and Huang, 1992; Perovic *et al.*, 1993). Both mechanisms are certainly active in the case of a HAADF image of an extended defect with the interband scattering effects being dominant.

It must be stressed that also the static disorder is known to produce an interband scattering in the states excited by the probe. This has been used to explain the HAADF intensity reduction in presence of a random strain field on atomic scale (Yu *et al.*, 2004; Grillo and Carlino, 2008).

However, when extended defects are dealt with, the typical scale length of the strain field is larger and the mechanism of interband scattering is not merely the effect of local disorder: while slowly varying strain fields induce a shift of the electron wave-function with the atomic column the random displacement with its rapid oscillation along the propagation direction produces mainly a reduction of the 1s excitation (Plamann and Hytch, 1999).

In spite of this general wisdom about strain effects even tiny difference in the intensities are often interpreted directly as due to compositional effects. The main reason for this could possibly lie in the lack of a quantitative evaluation of the size of strain effects.

For this reason I will analyse the case study of strained InGaAs/GaAs quantum wells (QWs) for which the chemical variation between the well and the barrier is generally considered to be the sole active contrast mechanism. A more accurate interpretation should otherwise consider that the operation of sample thinning to achieve electron transparency has induced surface relaxation at the upper and lower specimen surface. This phenomenon is known to influence the TEM contrast and the produced strain field can be predicted with very good accuracy (Wang 1994; De Caro *et al.*, 1997). For this reason it represent an ideal benchmark to test strain effects in HAADF. It is the aim of this work to evaluate quantitatively by both simulations and experiments such effects. In a first part of this work the phenomenology of the HAADF contrast as a function of different experimental parameters is described and discussed to exclude other possible contrast mechanisms. In a second part the experimental contrast is compared with multislice simulations in order to verify the quantitative match of the contrast profiles.

## Materials and Methods

A sample consisting of three pseudomorphic QWs of  $\text{In}_x\text{Ga}_{1-x}\text{As}$ , with In content  $x=0.05$ , 0.12 and 0.24 was grown by molecular beam epitaxy on GaAs (001) (Rubini *et al.*, 2006). The In content in the QWs was larger for the QW closer to the surface. The specimens for STEM experiments have been prepared in  $\langle 110 \rangle$  cross section geometry by mechanical grinding and ion milling, following a well established procedure (Grillo and Carlino, 2008). The relevant experiments

have been performed with a JEOL 2010F equipped by field emission gun and objective lens with a measured spherical aberration coefficient  $C_s = (0.47 \pm 0.01)$  mm, capable of a resolution, in HAADF, of 0.126 nm. All HAADF images were acquired by using an illumination convergence angle of 14 mrad and a detector collection angle of  $84 < 2\theta < 224$  mrad. HAADF images in  $\langle 110 \rangle$  zone axis were acquired for different STEM specimen thicknesses. The specimen thickness was measured by the projections methods and, where necessary, confirmed by convergent beam electron diffraction (Williams and Carter, 1996). Moreover the specimen tilt was also measured by stopping the beam on a selected position and acquiring by the CCD the relevant diffraction pattern. The calibration of the camera length of such pattern permits to directly extract the tilt angle from the distance between the centre of the transmitted beam circle and the centre of Laue zone.

## Results

Figure 1 shows a typical low magnification HAADF image of the sample along with the relevant line profile. All line profiles in this work have been obtained by a lateral averaging in the direction orthogonal to the growth direction to reduce the statistical noise and the influence of surface artefacts. The vacuum on the side of the specimen is clearly visible and it can be used for an evaluation of the effective dark counts. The intensity levels have been here expanded in order to give evidence to the features inside the sample. The most prominent feature is the presence of the three QWs with decreasing In concentrations at increasing distances from the surface. The difference in the In composition in the different QWs is visible as a different contrast to the GaAs barriers. In particular the inner QW has the lower intensity since it contains less In. A linear interpolation for the GaAs level has been also indicated with a dashed line as guide for the eyes.

In these conditions Figure 1 reveals a reduction of the HAADF intensity at one side of the outermost QW (with  $x=0.24$ ) and to a lower extent in the others. The size of the contrast due to these intensity dips is of the order of 20-30% of the QW contrast and is typically visible in the greyscale dynamic conditions used to appreciate

the QWs contrast.

The intensity drops below the average GaAs just at the side of the QW and then rises slowly until it reaches a flat value at more than 10 nm from the QW interface. This feature is particularly interesting because in a sample comprising only In,Ga and As (with no significant concentration of vacancies) no intensity level is expected below the GaAs level. It is also worth noting that the QW itself shows a relatively smooth profile at the interfaces.

I will concentrate on the origin of the intensity minimum in proximity of the interfaces of the QWs. To further characterize this effect a systematic variation of the imaging parameters has been performed. In particular we defined the contrast as:

$$C = \frac{I}{I_0}$$

$I_0$  is an intensity reference level obtained by linearly interpolating in the well region and its proximity the intensity profiles in the GaAs barriers. This procedure has been performed to eliminate the effects on the intensities given by the thickness increase moving toward the inner part of the sample.

A first series of experiments were performed by changing the specimen orientation by few mrad in order to evaluate whether these effects may be related to any miss-orientation of the specimen.

The intensity minimum at the interfaces varies in depth and position depending on the experimental conditions. By varying the angle of tilt the intensity minimum move from the left (referred to Figure 1a) to the right interface of the QW. For the intermediate value at the exact zone axis conditions, less pronounced minima are found at both interfaces.

This behaviour is well shown by Figure 2 in which the contrast profiles obtained for different specimen tilt conditions are shown. The figure refers to the In rich QW and the measured specimen thickness is in this case  $42 \pm 3$  nm. For large tilt the intensity minimum on the right toward the specimen edge increases while on the other interface the minimum is substituted by an intensity peak. Moreover for 9 mrad tilt the intensity in the QW region is roughly 30% higher than in the zone axis conditions.

A second kind of experiment was performed by changing the specimen thickness: in this case the relative importance of the dip in the intensity increases for decreasing thickness while it disappears almost completely for very thick samples (100 nm). Figure 3 shows the intensity contrast at the intensity minimum at exact zone axis conditions as a function of the specimen thick-

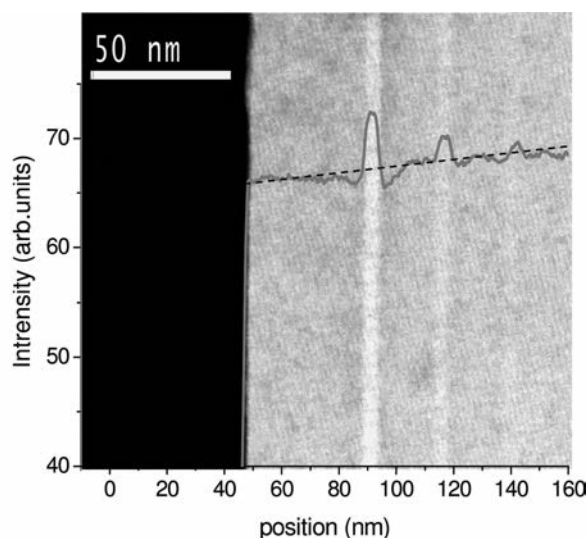


Figure 1. Low magnification HAADF cross sectional image of the sample in the InGaAs QWs region.

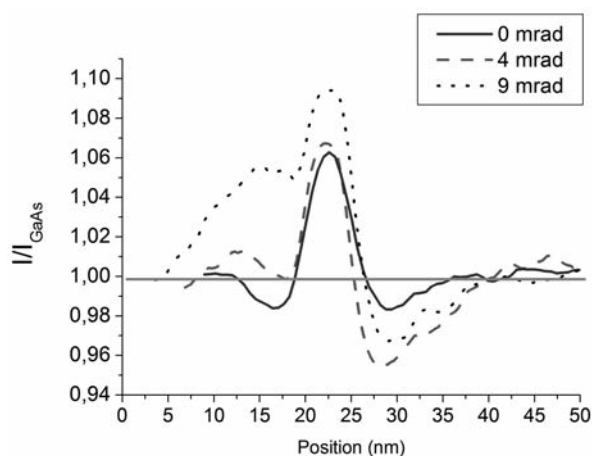


Figure 2. HAADF Intensity profiles of the sample for three different specimen tilt conditions in the QW with 24% In.



ness. A clear trend is visible confirming the reduction of the dip for increasing thickness. A fit with a rational function has been also added as a guide for the eyes. Summarizing, the experiments have produced the following evidences about the nature of the dip at the side of the QW.

- 1) The contrast of the intensity minima at the two interfaces can be varied by varying the tilt. In the cases of larger tilt one of the two minima can disappear while the other is strongly enhanced.
- 2) The contrast depth at the minimum decreases as the specimen thickness increases.

## Discussion

I have considered different contrast mechanism to explain the aforementioned evidences. The first is the presence of a large amount of point defects and composition anomalies at the interfaces of the QW. Yu *et al.* (Yu *et al.*, 2004) have already shown that Si implanted by ion bombardment can show a drastic reduction of its HAADF intensity. According to their work this reduction is mainly ascribable to a reduction of the channelling conditions. More in general this mechanism should be the dominant contrast mechanism at any point defect (Perovic *et al.*, 1993; Hillyard and Silcox, 1995).

The experimental results indicate however that the intensity variations at the InGaAs/GaAs interfaces cannot be ascribed to point defects. As a matter of facts, as the specimen undergoes a small misstilt outside the zone axis conditions the excitation of the columnar states and consequently the total HAADF intensity is reduced: however a point defect will not have any preferential direction and the effect of the tilt should be similar at both interfaces of the QW and for any tilt. It is then impossible to introduce any asymmetry in the intensity at the two interfaces of the QW, as actually observed, as a sole effect of tilting.

The strain relaxation induced by the thinning of the specimen is the simplest explanation of the experimental features.

An atomistic model for the relaxed structure is sketched in Figure 4. A section of the atomic structure comprising the QW and part of the barrier is represented. The x direction has been chosen in the growth direction of the structure and z along the electron propagation direction. The structure should be ideally continued along the

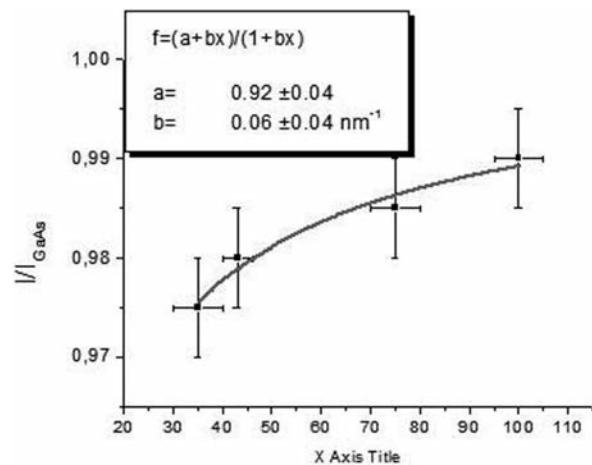


**Figure 3.** Plot of the Intensity at dip at the side of the QW normalized to GaAs level as a function of the specimen thickness. A plot with a rational function is also indicated.

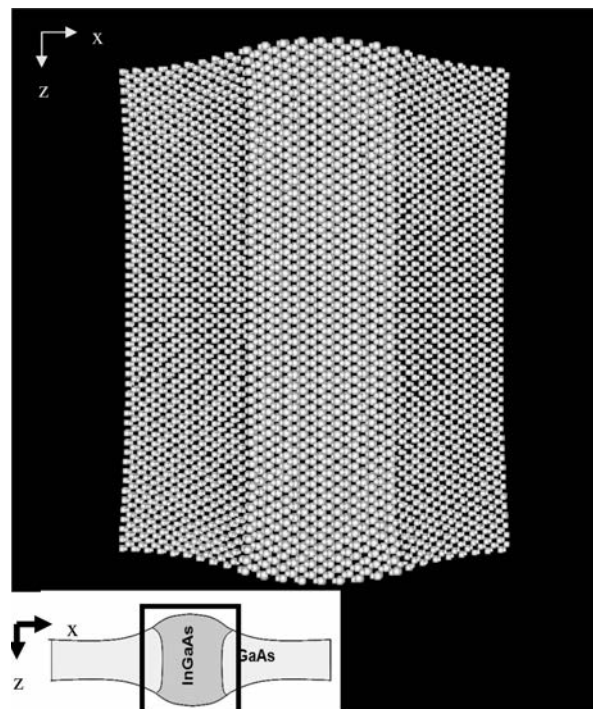


**Figure 4.** Atomistic model of the QW region with surface relaxation (Electron propagation direction is along z). The strain field has been enhanced by a factor 10 to provide a better visualization. A schematic of the QW structure is also shown. The region of the atomistic model is indicated by a rectangle.

positive and negative x direction, while the upper and lower free surfaces in the z direction are clearly visible with their deformed contour: the deformation have been enhanced by a factor 10 to provide a better visualization.

In order to understand this structure it is worth reminding that in pseudomorphic InGaAs/GaAs QWs grown on GaAs substrates, the difference between the lattice parameters of the two materials is accommodated by tetragonal deformation of the InGaAs lattice. In a thinned (S)TEM specimen, the free surfaces orthogonal to the electron propagation direction permit a relaxation of the strain at the InGaAs/GaAs interfaces. As a consequence of this relaxation both GaAs and InGaAs are largely bent in the zone of the interface closer to the free surfaces.

Since the HAADF intensity in zone axis condition is strongly enhanced by channeling, the bending at the first few nm of the sample surface with a consequent lower excitation of the 1s will produce an intensity dip in the zone of the interface. It is worth noting here that for sample thickness larger than 20-30 nm the bending of the exit (the lower one in Figure 4) free surface will not influence too much the overall intensity because the 1s state is typically largely absorbed within this distance.

A small tilt off the z.a. conditions can have the effect of partially compensating the effect at one interface of the QW while decreasing the excitation of columnar states on the other one, thus explaining evidence 1). Conversely when the sample thickness is increased, the relative weight of surface effects is reduced in agreement with evidence 2).

In order to give a quantitative account for this model by simulations, multislice calculations in the frozen phonon approximation (Kirkland, 1998) have been performed.

As a first step, the realistic strain model for the QW structure in presence of free surfaces has been calculated by means of the finite elements calculation [FEMLAB software ([www.femlab.com](http://www.femlab.com))]. The strain has been taken into account to calculate the atomic positions in an  $\text{In}_x\text{Ga}_{1-x}\text{As}/\text{GaAs}$  QW with  $x=0.24$ . Simulations have been performed for the case of specimen thickness of 40 nm. The multislice calculations have been performed by means of STEM\_CELL (Carlino and Grillo, 2007), a simulation package based on Kirkland routines (Kirkland, 1998) that permits to speed up the simulations by means of parallel

computing. In order to facilitate the simulation the atomistic model (like the one sketched in Figure 4) has been divided in sections used as input for the multislice. For each section of the atomistic model, the intensity has been calculated over a single unit cell in proximity of the centre of the selected section in order to reduce the effect of incorrect boundary conditions (see also (Grillo and Carlino, 2008)).

In order to ensure a correct sampling of the minimum spatial frequency, the samples has been taken about  $3 \times 3$  nm (depending on the local lattice parameter).

Figure 5 shows a direct comparison of simulation and experiment for a specimen thickness of  $42 \pm 3$  nm for the experiment and 40 nm for the simulation. Both images regard exact zone axis conditions.

The intensity shows a pronounced dip in proximity of the QW interfaces, while it slowly recovers the intensity of the unstrained case at larger distances. This behaviour is in excellent agreement with the experiments and is a demonstration that strain causes the observed variation of the HAADF intensity. Finally, it is worth noting that according to simulations inside the InGaAs QW the intensity is not flat but decreases at increasing distances from the centre. Unfortunately in exper-

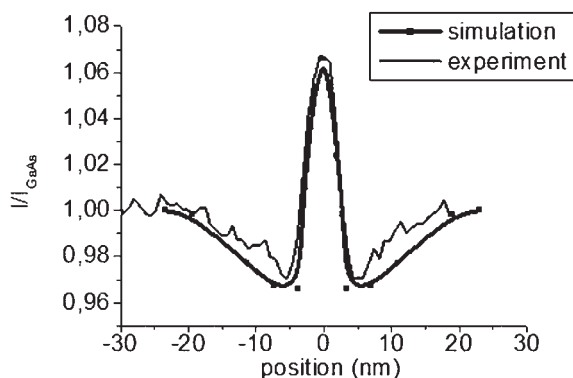


**Figure 5.** Simulated (solid line) and experimental (circles) intensity profiles for the 0.24% In QW. The specimen thickness is 40 nm for the simulation and  $42 \pm 3$  nm in the experiment. The simulation in dashed lines has been obtained scaling the intensity in the InGaAs layer for the Static Displacement correction as calculated in Grillo and Carlino (2008).

imental profiles this effect is completely superimposed to In segregation effects (Muraki *et al.*, 1992). Indeed experimental analysis of the lattice fringes distortion, performed on HRTEM images of the same sample, confirms that the In segregation accounts for the lineshape of the HAADF profile even without strain effects (Kret *et al.*, 2001). It is worth noting that the above considerations on strain effects can be extended to any other system where strain can be induced by the specimen thinning. The strain must be taken fully in account for a quantitative analysis of HAADF contrast experiments. It is further to be noticed that, because of the presence of strain, a sample tilt as small as 4 mrad can completely alter the intensity profile along the QW structure.

## Conclusions

In this article the contrast in STEM -HAADF imaging produced by of a strain field varying along the electron propagation direction has been studied. The case study was the surface strain relax-

ation in a thinned specimen comprising InGaAs/GaAs QWs. The advantage of this structure is that the phenomenon has been widely studied by TEM analysis and the strain field can be predicted with good accuracy. It has been demonstrated by the relatively good agreement of experiments and accurate frozen phonon simulations that the main contribution of surface relaxation is to add one or two intensity dips, depending on the specimen tilt, in the barrier region at the sides of the QWs and an artificial smoothing of the QW intensity profile. Both effects should be accounted for when performing quantitative compositional analysis.

## Acknowledgments

The author would also like to thank S. Rubini, G. Bais, A. Cristofoli, M. Piccin, F. Martelli, and A. Franciosi for providing the specimens; L. Palazzari and V. Rosato for the use of the parallel cluster of computers for the calculations. Moreover I would like to thank E. Carlino, F. Martelli, S. Frabboni and L. Felisari for critical reading of a related manuscript.

## References

- Amali A, Rez P, Cowley JM. High Angle Annular Dark Field Imaging of Stacking Faults. *Micron* 1997;28: 89-94.
- Anderson SC, Birkeland CR, Anstis GR, Cockayne DJH. An approach to quantitative compositional profiling at near-atomic resolution using high-angle annular dark field imaging, *Ultramicroscopy* 1997;69:83-103.
- Carlino E, Grillo V. Accurate and fast multislice simulation of HAADF image contrast by parallel computing *Microscopy of Semiconducting materials. Proceedings of the 15<sup>th</sup> Conference* 2007:177-80.
- Carlino E, Grillo V. Atomic-resolution quantitative composition analysis using scanning transmission electron microscopy Z-contrast experiments. *Phys Rev B* 2005;71:235-303.
- Coene W, Janssen G, Op de Beck M, Van Dyck D. Phase retrieval through focus variation for ultraresolution in field-emission TEM. *Phys Rev Lett* 1992; 29:3743-6.
- Cowley JM, Huang Y. De-channelling contrast in annular dark-field STEM. *Ultramicroscopy* 1992;40:171-80.
- De Caro L, Giuffrida A, Carlino E, Tapfer L. Effects of the Elastic Stress Relaxation on the HRTEM Image Contrast of Strained Heterostructures. *Acta Cryst A* 1997;53:168-74.
- Fitting L, Thiel S, Schmehl A, Mannhart J, Muller DA. Subtleties in ADF imaging and spatially resolved EELS: A case study of low-angle twist boundaries in SrTiO<sub>3</sub>. *Ultramicroscopy* 2006;106:1053-61.
- Grillo V, Carlino E. Influence of the static atomic displacement on atomic resolution Z-contrast imaging *Phys Rev B* 2008;77:054103.
- Hillyard S, Silcox J. Detector geometry, thermal diffuse scattering and strain effects in ADF STEM imaging *Ultramicroscopy* 1995;58:6-17.
- Kirkland EJ. *Advanced Computing in Electron Microscopy*. Plenum Press, New York, 1998.
- Klenov DO, Driscoll DC, Gossard AC, Stemmer S. Scanning transmission electron microscopy of ErAs nanoparticles embedded in epitaxial In<sub>0.53</sub>Ga<sub>0.47</sub>As layers. *Appl Phys Lett* 2005;86:111912.
- Kret S, Ruterana P, Rosenauer A, Gerthsen D. Extracting quantitative information from high resolution electron microscopy. *Phys Stat Sol B* 2001;227:247-95.
- Le Beau JM, Findlay SD, Allen LJ, Stemmer S. Quantitative Atomic Resolution Scanning Transmission Electron Microscopy *Phys Rev Lett* 2008;100:20610-1.
- Liu CP, Twesten RD, Gibson JM. High-angle annular dark-field imaging of self-assembled Ge islands on Si(0 0 1). *Ultramicroscopy* 2001;87:79-88.

- Liu CP, Preston A., Boothroyd CB, Humphreys CJ. Quantitative analysis of ultrathin doping layers in semiconductors using high-angle annular dark field images. *J Microscopy* 1999;194:171-82.
- Lopatin S, Chisholm MF, Pennycook SJ, Duscher G. Z-contrast imaging of dislocation cores at the GaAs/Si interface. *Appl Phys Lett* 2002;81:2728-30.
- Maccagnano-Zachera SE, Mkhoyan KA, Kirklanda EJ, Silcox J. Effects of tilt on high-resolution ADF-STEM imaging. *Ultramicroscopy* 2008;108:718-26.
- Muraki K, Fukatsu S, Shiraki Y, Ito R. Surface segregation of In atoms during molecular beam epitaxy and its influence on the energy levels in InGaAs/GaAs quantum wells. *Appl Phys Lett* 1992;61:557-9.
- Pennycook S.J, Jesson DE. High resolution incoherent imaging of crystals. *Phys Rev Lett* 1990;64:938-41.
- Perovic DD, Rossouw CJ, Howie A. Imaging elastic strains in high-angle annular dark field scanning transmission electron microscopy. *Ultramicroscopy* 1993;52:353-9.
- Plamann T, Hytch MJ. Tests on the validity of the atomic column approximation for STEM probe propagation. *Ultramicroscopy* 1999;78:153-61.
- Rafferty B, Nellist D, Pennycook J. On the origin of transverse incoherence in Z-contrast STEM. *J Electron Microscopy* 2001;50:227-33.
- Rubini S, Bais G, Cristofoli A, Piccin M, Duca R, Nacci C et al. Nitrogen-induced hindering of In incorporation in InGaAsN. *Appl Phys Lett* 2006;88:141923-5.
- Ruvimov S, Werner P, Scheerschmidt K, Gösele U, Heydenreich J, Richter U, et al. Structural characterisation of (In,Ga)As Quantum Dots in a GaAs matrix. *Phys Rev B* 1995;51:14766-9.
- Treacy MMJ, Gibson JM, Howie A. On elastic relaxation and long wavelength microstructures in spinodally decomposed  $\text{In}_x\text{Ga}_{1-x}\text{As}_y\text{P}_{1-y}$  epitaxial layers. *Philos Mag A* 1985;51:389-417.
- Van Dyck D, Op de Beeck M. A simple intuitive theory for electron diffraction. *Ultramicroscopy* 1996;64:99-107.
- Voyles PM, Grazul JL, Muller DA. Imaging individual atoms inside crystals with ADF-STEM. *Ultramicroscopy* 2003;96:251-73.
- Wang ZL. Dislocation contrast in high-angle hollow-cone dark-field TEM. *Ultramicroscopy* 1994;53:73-90.
- Williams DB, Carter CB. *Transmission electron Microscopy: A textbook for materials science*. Plenum Press, New York, 1996.
- Xin Y, Pennycook SJ, Browning ND, Nellist PD, Sivananthan S, Omnès F, et al. Direct observation of the core structures of threading dislocations in GaN. *Appl Phys Lett* 1998;72:2680-2.
- Yu Z, Muller DA, Silcox J. Effects of specimen tilt in ADF-STEM imaging of a-Si/c-Si interfaces. *Ultramicroscopy*, 2008;108:494-501.
- Yu Z, Muller D, Silcox J. Study of strain fields at a-Si/c-Si interface. *J Appl Phys* 2004;95:3362-71.